Volume 1 | Number 1 | Jan 2013 | Pages 1–100

Catalysis
Science &
Technology

www.rsc.org/catalysis

ROYAL SOCIETY
OF CHEMISTRY

ROYAL SOCIETY
OF CHEMISTRY

www.rsc.org/catalysis

Journal Name

COMMUNICATION

Enhanced Photocatalytic Hydrogen Production in Water under Visible Light Using Noble-Metal-Free Ferrous Phosphide as an Active Cocatalyst

Zijun Sun, Huanlin Chen, Qiang Huang, Pingwu Du*

For the first time, ferrous phosphide (Fe$_2$P) is used as an active noble-metal-free cocatalyst for photocatalytic H$_2$ production under visible light in water. The rate of H$_2$ production can be enhanced by more than 30 times through loading Fe$_2$P on CdS nanorod surfaces. Efficient charge transfer between the CdS and Fe$_2$P might be the key factor for the high photocatalytic activity.

Hydrogen (H$_2$) is considered an ideal energy carrier for future clean energy applications because of its high energy capacity and environmental friendliness.[1-2] Thus, solar-driven water splitting for H$_2$ production has attracted much attention for the past couple of decades.[3-7] Since Honda and Fujishima reported photocatalytic splitting of water on TiO$_2$ electrodes in 1972,[8] many efforts have focused on the development of TiO$_2$ materials for photocatalytic H$_2$ production in water. However, the obvious drawback of TiO$_2$ lies in its wide band gap. Among many other semiconductors, cadmium sulfide (CdS) has been demonstrated as a promising visible-light-driven photocatalyst for H$_2$ production (band gap ~2.4 eV) with good visible light absorption and high catalytic activity.[9-11] Generally, the photocatalytic efficiency of CdS is severely restricted by the photocorrosion and fast recombination of photoexcited charge carriers.[12-13] To solve this problem, many studies have loaded cocatalysts onto semiconductor surfaces to promote transfer processes of charge carriers.[12, 14-16] An appropriate cocatalyst can accommodate the photogenerated charge carriers, suppress charge recombination, and provide active sites to avoid back reactions.[6, 12, 17] By introducing noble metal cocatalysts, such as Pt,[15, 18-19] Ru,[20] and Pd,[21] high photocatalytic hydrogen production efficiencies have been achieved. However, considering the practicality in applications, it is necessary to develop novel active cocatalysts made of inexpensive and earth-abundant materials for an artificial photocatalytic H$_2$ production system. Some examples have been reported in previous studies, such as MoS$_2$,[16, 22] Ni,[23] NiS,[17] Ni(OH)$_2$,[12] and CoS.[24-25]

Catalytic reduction of protons to produce H$_2$ by Fe-based

hydrogenases is an important biological reaction. Inspired by nature, many Fe-based hydrogenase mimic complexes have been studied for photocatalytic hydrogen production,[26-28] but very few Fe-based heterogeneous materials have been reported for this purpose.[29-30] Fe$_2$P, a material made of earth-abundant elements, has been widely used in lithium-ion batteries due to its crucial role in enhancing the electronic conductivity.[31-32] Only recently, it was found that Fe$_x$P (x=1 or 2) can be used as a good electrocatalyst for H$_2$ production.[33-35] However, the use of Fe$_2$P as a cocatalyst for photocatalytic H$_2$ evolution under visible light has not received prior investigation. Herein, we report for the first time that low-cost Fe$_2$P can be used as a cocatalyst on CdS nanorods (CdS NRs) for photocatalytic H$_2$ production in water.
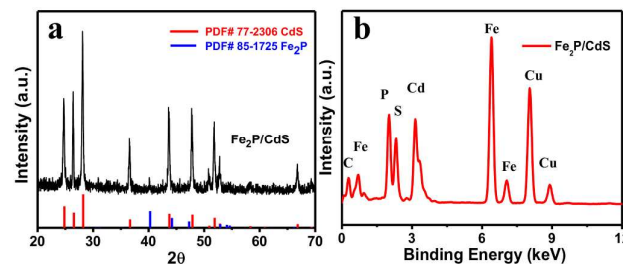
Figure 1. (a) Powder XRD patterns of CdS, Fe$_2$P/CdS (30 wt%), and Fe$_2$P samples. (b) EDX spectrum of Fe$_2$P/CdS (30 wt%) sample.

In this present study, Fe$_2$P nanoparticles were facilely synthesized (see experimental details) and loaded onto the CdS surface. Under optimal conditions, the H$_2$ evolution rate reached 186 µmol h^{-1} mg^{-1} (λ > 420 nm) and the apparent quantum efficiency (AQY) was ~15% at 450 nm. The aforementioned H$_2$ rate is more than 30 times higher than that of bare CdS NRs under the same condition.

To determine the crystallinities of the as-prepared composites, the XRD patterns of CdS NRs, Fe$_2$P/CdS NRs (30 wt%), and Fe$_2$P were measured and the results are shown in Figure S1 and Figure 1a. The CdS NRs (Figure S1a) shows typical peaks at 24.8°, 26.5°, 28.2°, 36.7°, 43.7°, 47.9°, 51.9°, and 66.8°, which were indexed respectively to the (100), (002), (101), (102), (110), (103), (112), and (203) planes of hexagonal CdS (PDF#77-2306).[13] For pure Fe$_2$P (Figure S1b), the diffraction peaks located at 40.3°, 44.2°, 47.3°, 52.9°, 54.1°, and 54.6° can be assigned to hexagonal Fe$_2$P (PDF#85-

Key Laboratory of Materials for Energy Conversion, Chinese Academy of Sciences, Department of Materials Science and Engineering, iChEM (Collaborative Innovation Center of Chemistry for Energy Materials), University of Science and Technology of China (USTC), 96 Jinzhai Road, Hefei, Anhui Province, 230026, P. R. China. Fax: 86-551-63606207. Email: dupingwu@ustc.edu.cn

1725). Moreover, the typical diffraction peaks of Fe_2P and CdS were both shown in Fe_2P/CdS NRs composite samples and no other impurities were detected, indicating the good phase purity of the Fe_2P/CdS NRs composite. The EDX data in Figure 1b further confirmed the existence of only Cd, S, Fe, and P elements in the Fe_2P/CdS NRs sample. The observed Cu element was from the copper grids.
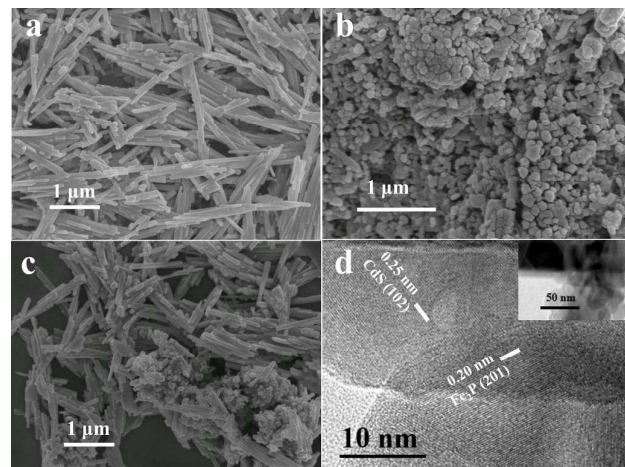

Figure 2. SEM images of (a) CdS, (b) Fe_2P, and (c) 30 wt% Fe_2P/CdS; (d) HRTEM image of 30 wt% Fe_2P/CdS (Insert: Low-magnification TEM image).

The morphologies of CdS NRs, Fe_2P, and Fe_2P/CdS NRs (30 wt%) were examined by scanning electron microscopy (SEM). It can be seen from Figure 2a that CdS NRs have typically smooth surfaces throughout the entire rods with average diameter of 40~90 nm and average length of 0.3~2.0 μm. In the Fe_2P sample, small nanoparticles of size ~100 nm were observed aggregated together (Figure 2b). In Figure 2c, Fe_2P nanoparticles were obviously in contact with the surface of CdS NRs to form a semiconductor-cocatalyst structure. More microstructural details of the interfacial region in Fe_2P/CdS NRs composite were observed in the HRTEM image (Figure 2d). The crystalline lattice spacing with ~0.20 nm can be assigned to the (201) plane of hexagonal Fe_2P and the lattice spacing with ~0.25 nm corresponds to the (102) plane of hexagonal CdS. The high-resolution image clearly showed that some Fe_2P nanoparticles were in close contact with the CdS NRs.

The effect of Fe_2P as an active cocatalyst in improving photocatalytic activity of CdS NRs was studied by monitoring photocatalytic H_2 evolution in a system containing 1.0 mg photocatalyst and 0.5 M ascorbic acid in aqueous solution at pH = 4.2 (Figure 3a). Based on the results, Fe_2P alone showed no appreciable H_2 production under visible light irradiation (λ > 420 nm), indicating that Fe_2P is not an active photocatalyst. In contrast, the Fe_2P/CdS NRs gave a H_2 evolution rate of 186 μmol h^{-1} mg^{-1}, which is more than 30 times higher than that of pure CdS NRs (6 μmol h^{-1} mg^{-1}). Furthermore, the mixture of Fe_2P+CdS NRs (30 wt%) without heat treatment yielded a H_2 production rate of ~140 μmol h^{-1} mg^{-1}, which is less than the Fe_2P/CdS NRs sample with heat treatment, probably due to the increasing compact contact between Fe_2P and CdS NRs upon heat treatment. The dependence of different amounts of Fe_2P on the photocatalytic H_2 evolution rate of Fe_2P/CdS NRs is shown in Figure 3b. The optimal content of Fe_2P/CdS NRs was determined to be 30 wt%, which gives a H_2 production rate of 186 μmol h^{-1} mg^{-1}. A higher content of Fe_2P led

to a decreasing rate, probably because the excess Fe_2P covering the surface of CdS hampered the incident light and prevented the generation of electrons from CdS NRs.[36-37] Moreover, the photocatalytic activities of Fe_2P using different electron donors (0.5 M ascorbic acid, pH=4.2; 10% lactic acid; 10% TEOA; and 0.25 M Na_2S/0.35 M Na_2SO_3) were also investigated and the results are shown in Figure S2. Pure CdS showed very low photocatalytic hydrogen evolution rate in all these electron donors. But after loading Fe_2P on it, the photocatalytic hydrogen evolution rate increased more than 30 times for ascorbic acid, lactic acid and TEOA, indicating that Fe_2P is a good cocatalyst. However, there was only 4 times higher for Na_2SO_3/Na_2S electron donors, indicating that the alkaline condition might inhibit the activity of Fe_2P.
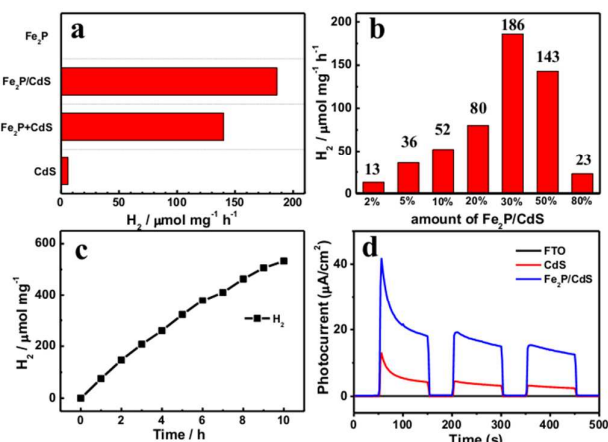
Figure 3. (a) Photocatalytic H_2 production rates of CdS, Fe_2P+CdS (30 wt%), Fe_2P/CdS (30 wt%), and Fe_2P samples over 3 hours. (b) Photocatalytic H_2 production rates of different amounts of Fe_2P on CdS NRs. (c) Time courses of H_2 production under monochromatic 450 nm (±5 nm) light irradiation of Fe_2P/CdS (30 wt%). (d) Transient photocurrent responses of blank FTO, CdS, and Fe_2P/CdS (30 wt%).

The performance of Fe_2P/CdS NRs (30 wt%) for photocatalysis was measured under a 300 W Xe lamp with a 450 nm (± 5 nm) band-pass filter to investigate the catalytic durability and apparent quantum yield (AQY) (Figure 3c). With no consideration of H_2 dissolution in the solvent, the amount of H_2 reached ~532 μmol and the H_2 evolution rate showed only a slight decrease after 10 hours of illumination, suggesting the good durability of Fe_2P/CdS NRs samples for photocatalytic H_2 production. Moreover, the SEM image of the Fe_2P/CdS NRs sample after visible light irradiation was also measured, as shown in Figure S3. Comparing with the image before photocatalytic reaction in Figure 2c, there is no significant difference of the SEM image after 10 hours of reaction. This result further indicates the good stability of Fe_2P/CdS NRs during this H_2 production reaction. In addition, the initial AQY reached ~15% at 450 nm (±5 nm), revealing that Fe_2P/CdS NRs composite has good efficiency for photocatalysis in aqueous solution.

To investigate why Fe_2P is able to enhance the photocatalytic activity, photoelectrochemical experiments were performed to study the transfer of charge carriers in the photocatalysts under visible light irradiation. The experiments were run in 0.5 M Na_2SO_4 solution using CdS and Fe_2P/CdS coated FTO as the working electrode, an Ag/AgCl electrode as a reference, and Pt wire as the counter electrode. As shown in Figure 3d, the Fe_2P/CdS NRs sample showed much higher photocurrents under chopped light than bare

CdS NRs by themselves. This observation revealed that the charge transfer process is more efficient in the Fe₂P/CdS NRs sample than in pure CdS NRs, which might explain the improvement in photocatalytic activity according to previous studies.[12, 38]

The photophysical properties of the Fe₂P/CdS NRs and CdS NRs were further measured by UV-vis-NIR spectroscopy and photoluminescence (PL) spectroscopy. As shown in Figure 4a, CdS NRs showed a sharp absorption edge at around 520 nm, corresponding to a band gap of ~2.4 eV, which is consistent with the band gap of CdS reported in the literature.[10-11, 13] Fe₂P showed a typical metallic character,[32, 39] which can not be directly used for visible-light-driven H₂ production. After loading Fe₂P on CdS NRs, the increasing absorption (520-1200 nm) can be obviously seen with the increasing content of Fe₂P. In addition, the composite still showed an absorption edge located at around 520 nm, indicating that Fe₂P did not dope into the CdS crystal lattice to change its band gap. The PL spectra are shown in Figure 4b to further confirm the charge transfer process in the Fe₂P/CdS NRs composite. Based on the PL data, the CdS material shows two distinct emission bands at about 504 nm and 700 nm under an excitation wavelength of 405 nm. The former one is probably associated with near-band-edge emission while the latter one is attributed to surface defects.[40-41] According to the literature, photogenerated carriers are easily transferred to the abundant surface states in which the electrons are not available for H₂ evolution.[40] Fe₂P by itself shows no PL intensity under an excitation wavelength of 405 nm. After loading Fe₂P on CdS, the PL intensity of these two emission bands is much weaker than that of CdS, suggesting a fast photoinduced electron transfer process in Fe₂P/CdS NRs. Moreover, the weaker intensity of emission band at 700 nm also suggests that most of the surface states are passivated,[40-41] making the electrons energetically favorable for photocatalytic H₂ evolution.

Based on the above results, it is obviously that the as-synthesized Fe₂P shows a metallic character and shows no photocatalytic hydrogen activity. With the introduction of Fe₂P on CdS, a typical metal-semiconductor interfaces was thus created. Thus, the electrons could effectively transfer from semiconductor to metallic cocatalyst through the interfaces, promote the separation of the photogenerated electron-holes. Moreover, we also found that loading Fe₂P could passivate the defects on the CdS surface, which also can improve the photocatalytic activity.
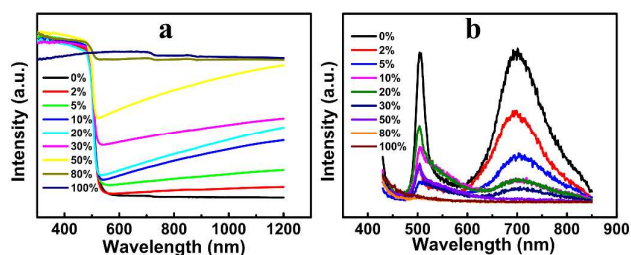
Figure 4. (a) UV-vis diffuse reflectance spectra and (b) Photoluminescence (PL) spectra under an excitation wavelength of 405 nm of Fe₂P/CdS samples with different content of Fe₂P.

Conclusions

In conclusion, Fe₂P nanomaterial was found to be an active cocatalyst on CdS NRs surface for photocatalytic H₂ production in water under visible light. Under optimal conditions, the corresponding hydrogen production rate reached 186 μmol h⁻¹ mg⁻¹

and the AQY is ~15% at 450 nm. The aforementioned rate is more than 30 times higher than that of pure CdS NRs, indicating a highly improved activity for photocatalysis. Since the Fe₂P cocatalyst is made of cheap and abundant elements, it holds great promise for more applications.

Notes and references

1   H. B. Gray, *Nat. Chem.* 2009, **1**.
2   M. S. Dresselhaus, I. L. Thomas, *Nature* 2001, **414**, 332-337.
3   X. B. Chen, S. H. Shen, L. J. Guo, S. S. Mao, *Chem. Rev.* 2010, **110**, 6503-6570.
4   T. Hisatomi, J. Kubota, K. Domen, *Chem. Soc. Rev.* 2014, **43**, 7520-7535.
5   H. L. Wang, L. S. Zhang, Z. G. Chen, J. Q. Hu, S. J. Li, Z. H. Wang, J. S. Liu, X. C. Wang, *Chem. Soc. Rev.* 2014, **43**, 5234-5244.
6   P. Du, R. Eisenberg, *Energy Environ. Sci.* 2012, **5**, 6012-6021.
7   A. Kudo, Y. Miseki, *Chem. Soc. Rev.* 2009, **38**, 253-278.
8   A. Fujishima, K. Honda, *Nature* 1972, **238**, 37-38.
9   F. Wen, C. Li, *Acc. Chem. Res.* 2013, **46**, 2355-2364.
10   M. Matsumura, S. Furukawa, Y. Saho, H. Tsubomura, *J. Phys. Chem.* 1985, **89**, 1327-1329.
11   J. F. Reber, M. Rusek, *J. Phys. Chem.* 1986, **90**, 824-834.
12   Z. P. Yan, X. X. Yu, A. L. Han, P. Xu, P. W. Du, *J. Phys. Chem. C* 2014, **118**, 22896-22903.
13   Z. Sun, Q. Yue, J. Li, J. Xu, H. Zheng, P. Du, *J. Mater. Chem. A* 2015, **3**, 10243-10247.
14   J. H. Yang, D. G. Wang, H. X. Han, C. Li, *Acc. Chem. Res.* 2013, **46**, 1900-1909.
15   J. H. Yang, H. J. Yan, X. L. Wang, F. Y. Wen, Z. J. Wang, D. Y. Fan, J. Y. Shi, C. Li, *J. Catal.* 2012, **290**, 151-157.
16   X. Zong, H. J. Yan, G. P. Wu, G. J. Ma, F. Y. Wen, L. Wang, C. Li, *J. Am. Chem. Soc.* 2008, **130**, 7176-7177.
17   W. Zhang, Y. B. Wang, Z. Wang, Z. Y. Zhong, R. Xu, *Chem. Commun.* 2010, **46**, 7631-7633.
18   E. Elmalem, A. E. Saunders, R. Costi, A. Salant, U. Banin, *Adv. Mater.* 2008, **20**, 4312-4317.
19   L. A. Silva, S. Y. Ryu, J. Choi, W. Choi, M. R. Hoffmann, *J. Phys. Chem. C* 2008, **112**, 12069-12073.
20   J. Sato, N. Saito, Y. Yamada, K. Maeda, T. Takata, J. N. Kondo, M. Hara, H. Kobayashi, K. Domen, Y. Inoue, *J. Am. Chem. Soc.* 2005, **127**, 4150-4151.
21   T. Sreethawong, S. Yoshikawa, *Catal. Commun.* 2005, **6**, 661-668.
22   X. Zong, G. P. Wu, H. J. Yan, G. J. Ma, J. Y. Shi, F. Y. Wen, L. Wang, C. Li, *J. Phys. Chem. C* 2010, **114**, 1963-1968.
23   Y. Yamada, T. Miyahigashi, H. Kotani, K. Ohkubo, S. Fukuzumi, *Energy Environ. Sci.* 2012, **5**, 6111-6118.
24   Z. M. Yu, J. L. Meng, J. R. Xiao, Y. Li, Y. D. Li, *Int. J. Hydrogen Energy* 2014, **39**, 15387-15393.
25   Y. S. Zhu, Y. Xu, Y. D. Hou, Z. X. Ding, X. C. Wang, *Int. J. Hydrogen Energy* 2014, **39**, 11873-11879.
26   J. X. Jian, Q. Liu, Z. J. Li, F. Wang, X. B. Li, C. B. Li, B. Liu, Q. Y. Meng, B. Chen, K. Feng, C. H. Tung, L. Z. Wu, *Nat. Commun.* 2013, **4**.

27 C. B. Li, Z. J. Li, S. Yu, G. X. Wang, F. Wang, Q. Y. Meng, B. Chen, K. Feng, C. H. Tung, L. Z. Wu, *Energy Environ. Sci.* 2013, **6**, 2597-2602.

28 N. Wang, M. Wang, Y. Wang, D. H. Zheng, H. X. Han, M. S. G. Ahlquist, L. C. Sun, *J. Am. Chem. Soc.* 2013, **135**, 13688-13691.

29 J. S. Jang, H. G. Kim, V. R. Reddy, S. W. Bae, S. M. Ji, J. S. Lee, *J. Catal.* 2005, **231**, 213-222.

30 F. Gartner, B. Sundararaju, A. E. Surkus, A. Boddien, B. Loges, H. Junge, P. H. Dixneuf, M. Beller, *Angew. Chem. Int. Ed.* 2009, **48**, 9962-9965.

31 C. W. Kim, J. S. Park, K. S. Lee, *J. Power Sources* 2006, **163**, 144-150.

32 M. S. Song, D. Y. Kim, Y. M. Kang, Y. I. Kim, J. Y. Lee, H. S. Kwon, *J. Power Sources* 2008, **180**, 546-552.

33 Z. P. Huang, C. C. Lv, Z. Z. Chen, Z. B. Chen, F. Tian, C. Zhang, *Nano Energy* 2015, **12**, 666-674.

34 P. Jiang, Q. Liu, Y. Liang, J. Tian, A. M. Asiri, X. Sun, *Angew. Chem. Int. Ed.* 2014, **53**, 12855-12859.

35 Z. Zhang, B. Lu, J. Hao, W. Yang, J. Tang, *Chem. Commun.* 2014, **50**, 11554-11557.

36 J. Zhang, S. Z. Qiao, L. F. Qi, J. G. Yu, *Phys. Chem. Chem. Phys.* 2013, **15**, 12088-12094.

37 X. W. Wang, L. C. Yin, G. Liu, *Chem. Commun.* 2014, **50**, 3460-3463.

38 S. Cao, Y. Chen, C. J. Wang, P. He, W. F. Fu, *Chem. Commun.* 2014, **50**, 10427-10429.

39 M. Sharon, G. Tamizhmani, *J. Mater. Sci.* 1986, **21**, 2193-2201.

40 L. Huang, X. L. Wang, J. H. Yang, G. Liu, J. F. Han, C. Li, *J. Phys. Chem. C* 2013, **117**, 11584-11591.

41 S. Q. Liu, Z. Chen, N. Zhang, Z. R. Tang, Y. J. Xu, *J. Phys. Chem. C* 2013, **117**, 8251-8261.

Table of contents

For the first time, ferrous phosphide (Fe_2P) is used as an active noble-metal-free cocatalyst for photocatalytic H_2 production under visible light in water. The rate of H_2 production can be enhanced by more than 30 times with Fe_2P on CdS nanorod surfaces.